to the presence or absence of *MYCN* amplification. Figure 3a shows that the 5-year survival rates of patients with GGSs ($n=18$), GGWs ($n=33$) and GGPs ($n=25$) tumors were 89, 85 and 53%, respectively, whereas those of patients with GGSa ($n=5$), GGWa ($n=3$) and GGPa ($n=28$) tumors involving *MYCN* amplification were 0, 33 and 34%, respectively (Figure 3b). We then further examined the survival curves of patients with *MYCN*-nonamplified tumors in young (<1-year-old) and old (⩾1-year-old) patients. Figure 3c shows the 5-year survival rates of 88, 86 and 67% in GGWs ($n=24$), GGSs ($n=7$) and GGPs ($n=3$) tumors, respectively, among young patients, whereas they were 76, 91 and 51% in GGWs ($n=9$), GGSs ($n=11$) and GGPs ($n=22$) tumors, respectively, among old patients (Figure 3d). The former pattern was similar to that in MS-detected tumors, which had high percentages of GGW tumors, whereas the latter contained high incidences of GGP tumors.

**Table 1** Five-year overall survival rates of the patients with each genomic subgroup of sporadic neuroblastomas

| | N | *5-Year OS (%)* |
|---|---|---|
| *GGS* | | |
| GGSa | 5 | 0 |
| GGSs | 18 | 89 |
| *GGP* | | |
| GGP1a | 22 | 44 |
| GGP1s | 2 | 0 |
| GGP2a | 4 | 0 |
| GGP2s | 5 | 40 |
| GGP3a | 1 | 0 |
| GGP3s | 15 | 59 |
| GGP4a | 1 | 0 |
| GGP4s | 3 | 67 |
| *GGW* | | |
| GGW1a | 0 | — |
| GGW1s | 0 | — |
| GGW2a | 0 | — |
| GGW2s | 1 | 100 |
| GGW3a | 0 | — |
| GGW3s | 3 | 100 |
| GGW4a | 1 | 0 |
| GGW4s | 23 | 87 |
| GGW5a | 2 | 50 |
| GGW5s | 6 | 67 |

Abbreviations: GGP, partial chromosomal gains/losses genomic group; GGS, silent genomic group; GGW, whole gains and/or losses genomic group; OS, overall survival rate.

*Segregation of the prognosis of sporadic neuroblastomas with a single copy of MYCN by genomic and molecular signatures*

Recently, we have generated a clinically useful cDNA microarray carrying 200 genes that predicts the prognosis of neuroblastomas with an accuracy rate of 89% (Ohira *et al.*, 2005). The univariate analysis of 112 sporadic neuroblastomas showed that both genomic signatures (GGP vs GGW+GGS, $P=0.003$) and molecular signatures (posterior value<0.5 vs ⩾0.5, $P<0.001$) were highly significant prognostic indicators, like other variables including age ($P=0.006$), stage ($P<0.001$), tumor origin ($P=0.001$), *TrkA* expression ($P=0.004$), Shimada classification ($P<0.001$) and *MYCN* amplification ($P<0.001$; Table 2). In addition, genomic signature was a prognostic factor independent from molecular signature, age and tumor origin, although it showed no prognostic significance when stage, Shimada classification, or *MYCN* amplification was controlled (Table 2). Even in sporadic neuroblastomas with a single copy of *MYCN*, the highest significance according to the univariate analysis was given to molecular signature ($P=0.002$), followed by tumor origin ($P=0.006$) and genomic signature ($P=0.010$; Table 2). The multivariate analysis also showed that genomic signature was a prognostic indicator independent from molecular signature or tumor origin (Table 2). As shown in Figure 4, our in-house expression microarrays segregated the survival curves of patients with sporadic tumors lacking *MYCN* amplification (GGSs+GGPs+GGWs) into the favorable (94%, $n=17$) and unfavorable (42%, $n=13$) prognosis groups ($P=0.001$).

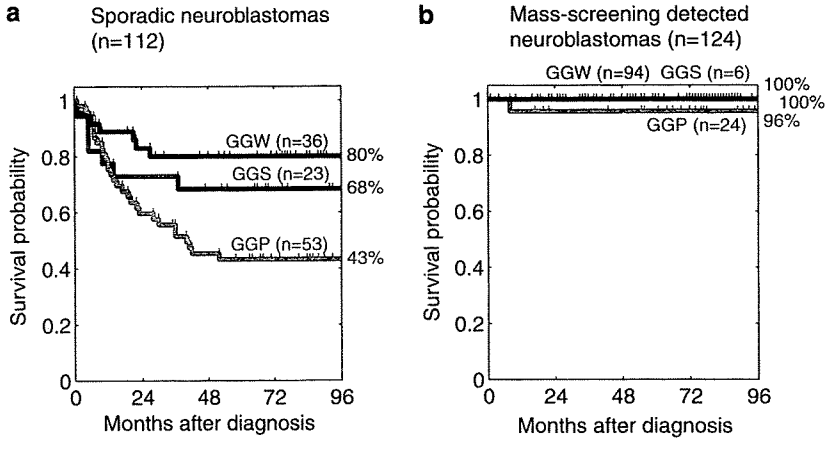


**Figure 2** Kaplan–Meier survival curves in three genomic groups (GGS, GGP and GGW) based on array-CGH. (**a**) Sporadic neuroblastomas: GGS vs GGP: $P=0.109$, GGS vs GGW: $P=0.320$ and GGP vs GGW: $P=0.002$. (**b**) Mass screening-detected neuroblastomas: GGS vs GGP: $P=1.000$, GGS vs GGW: $P=1.000$ and GGP vs GGW: $P=1.000$.

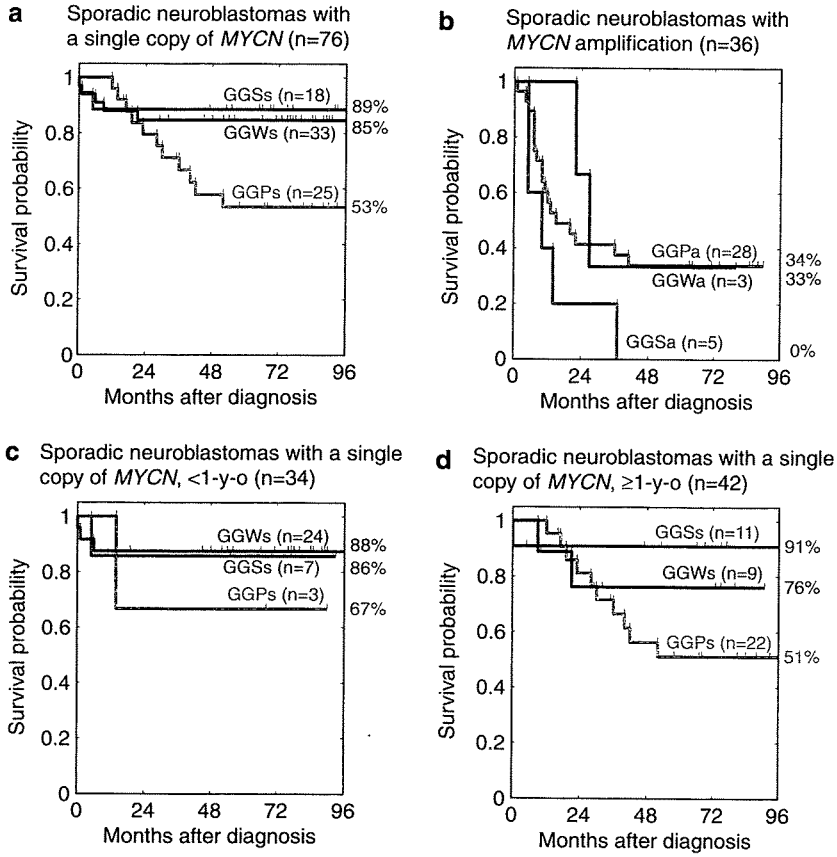


**Figure 3** Kaplan–Meier survival curves in three genomic groups (GGS, GGP and GGW) of sporadic neuroblastomas based on array-CGH. (**a**) Sporadic neuroblastomas with a single copy of *MYCN* GGS vs GGP: $P=0.035$, GGS vs GGW: $P=0.736$ and GGP vs GGW: $P=0.033$. (**b**) Sporadic neuroblastomas with *MYCN* amplification GGS vs GGP: $P=0.104$, GGS vs GGW: $P=0.156$ and GGP vs GGW: $P=0.642$. (**c**) Sporadic neuroblastomas with a single copy of *MYCN* in patients under 1 year of age GGS vs GGP: $P=1.000$, GGS vs GGW: $P=0.919$ and GGP vs GGW: $P=0.412$. (**d**) Sporadic neuroblastomas with a single copy of *MYCN* in patients over 1 year of age. GGS vs GGP: $P=0.063$, GGS vs GGW: $P=0.478$ and GGP vs GGW: $P=0.481$.

## Discussion

The present array-CGH analysis revealed the whole feature of the genomic abnormality patterns of sporadic and MS-detected neuroblastomas. The patterns of genomic aberrations in MS-detected neuroblastomas are similar to those in sporadic tumors, suggesting that they are genetically genuine neuroblastomas which are similar to sporadic tumors found in patients under 1 year of age. Indeed, both of them have a high tendency to regress spontaneously. The exceptions we found are that the incidence of GGPs tumors is relatively higher in MS-detected tumors than in sporadic tumors found among young patients and that their clinical outcome is very good.

BAC array-based aCGH analyses have defined several minimal critical regions of gains and losses in 1p, 2p and 11q. These included minimal losses in 10 Mb regions of 1p36.3 (1pter to RP11-199O1, *D1S244*) and 11q23 (from RP11-42L18 to RP11-45N4). The 2 Mb region in 1p36.2–36.3 detected by a BAC clone RP11-219F4 (*D1S507*) exhibited highest deletion frequency of 32%. By combining the expression data obtained by the in-house microarrays harboring approximately 5340 genes derived from primary neuroblastomas, several candidate genes including *CHD5* at 1p36 (Bagchi *et al.*, 2007) as well as *Survivin* at 17q25 (Islam *et al.*, 2000) were identified as lowly and highly expressed genes in neuroblastomas with advanced stages, respectively (manuscript in preparation). The amplicon surrounding the *MYCN* locus was ranged from 2.4 Mb proximal (*G14110*) to 5 Mb distal (*D2S387*) of *MYCN* itself and gains were further extended to wider range, from 2pter to 2p11.

To date, the presence of the GGS subgroup with very silent aberrations of the tumor genome has never been verified definitely. The distribution of GGS tumors is very unique; namely, they are present in both MS detected and sporadic tumors removed from the patients under 1 year of age. They are also found in tumors obtained from the patients over 1 year of age, and some of them possess *MYCN* amplification. Furthermore, GGS tumors mostly show diploid karyotype. These facts suggest that GGSs tumors might represent neuroblastoma at an early stage of carcinogenesis with early oncogenic hit(s), which later develop to GGP or

**Table 2** Univariate and multivariate analyses of genomic and molecular signature as well as other prognostic factors in sporadic neuroblastomas

| | *Sporadic NBLs (all cases)* | | | | *Sporadic NBLs (MYCN, single copy)* | | | |
|---|---|---|---|---|---|---|---|---|
| | N | P | *HR* | *CI* | N | P | *HR* | *CI* |
| Genomic signature (GGP vs GGW+GGS) | 53 vs 59 | 0.003 | 2.59 | (1.36, 4.90) | 25 vs 51 | 0.010 | 3.41 | (1.32, 8.82) |
| Molecular signature (posterior <0.5 vs ⩾0.5) | 22 vs 18 | <0.001 | 11.15 | (2.52, 49.35) | 13 vs 17 | 0.002 | 14.05 | (1.72, 114.89) |
| Age (⩾1-year old vs <1-year old) | 74 vs 38 | 0.006 | 2.67 | (1.24, 5.77) | 42 vs 34 | 0.070 | 2.47 | (0.88, 6.96) |
| Stage (3, 4 vs 1, 2, 4s) | 73 vs 38 | <0.001 | 4.92 | (1.93, 12.54) | 38 vs 37 | 0.038 | 2.80 | (1.00, 7.88) |
| Origin (adrenal vs nonadrenal) | 72 vs 40 | 0.001 | 3.22 | (1.43, 7.25) | 41 vs 35 | 0.006 | 4.59 | (1.33, 15.85) |
| TRKA expression (low vs high) | 52 vs 36 | 0.004 | 3.37 | (1.36, 8.34) | 24 vs 36 | 0.766 | 1.21 | (0.34, 4.31) |
| Shimada (unfavorable vs favorable) | 39 vs 37 | <0.001 | 4.54 | (1.71, 12.07) | 14 vs 36 | 0.668 | 1.37 | (0.33, 5.75) |
| MYCN (amplification vs single copy) | 36 vs 75 | <0.001 | 3.98 | (2.16, 7.35) | — | — | — | — |
| Genomic signature (GGP vs GGW+GGS) | 15 vs 25 | 0.045 | 2.89 | (1.01, 8.30) | 8 vs 22 | 0.031 | 5.46 | (1.09, 27.40) |
| Molecular signature (posterior<0.5 vs ⩾0.5) | 22 vs 18 | 0.002 | 7.52 | (1.69, 33.38) | 13 vs 17 | 0.034 | 7.41 | (0.90, 60.87) |
| Genomic signature (GGP vs GGW+GGS) | 53 vs 59 | 0.048 | 1.99 | (1.05, 3.78) | 25 vs 51 | 0.055 | 2.85 | (1.10, 7.36) |
| Age (⩾1-year old vs <1-year old) | 74 vs 38 | 0.132 | 1.88 | (0.87, 4.06) | 42 vs 34 | 0.549 | 1.44 | (0.51, 4.05) |
| Genomic signature (GGP vs GGW+GGS) | 53 vs 58 | 0.416 | 1.34 | (0.71, 2.54) | 25 vs 50 | 0.098 | 2.61 | (1.01, 6.76) |
| Stage (3, 4 vs 1, 2, 4s) | 73 vs 38 | 0.005 | 4.06 | (1.60, 10.34) | 38 vs 37 | 0.496 | 1.56 | (0.56, 4.40) |
| Genomic signature (GGP vs GGW+GGS) | 53 vs 59 | 0.012 | 2.23 | (1.18, 4.23) | 25 vs 51 | 0.015 | 3.19 | (1.23, 8.26) |
| Origin (adrenal vs non-adrenal) | 72 vs 40 | 0.006 | 2.78 | (1.24, 6.26) | 41 vs 35 | 0.008 | 4.30 | (1.24, 14.88) |
| Genomic signature (GGP vs GGW+GGS) | 41 vs 47 | 0.079 | 2.17 | (0.96, 4.95) | 18 vs 42 | 0.050 | 3.75 | (1.06, 13.33) |
| TRKA expression (low vs high) | 52 vs 36 | 0.078 | 2.34 | (0.95, 5.79) | 24 vs 36 | 0.727 | 0.79 | (0.22, 2.80) |
| Genomic signature (GGP vs GGW+GGS) | 53 vs 58 | 0.236 | 1.53 | (0.81, 2.90) | — | — | — | — |
| MYCN (amplification vs single copy) | 36 vs 75 | <0.001 | 3.30 | (1.79, 6.08) | — | — | — | — |

Abbreviations: CI, confidence interval; GGP, partial chromosomal gains/losses genomic group; GGS, silent genomic group; GGW, whole gains and/or losses genomic group; HR, hazard ratio; *N*, sample number; NBLs, neuroblastomas; *P*, *P*-value.

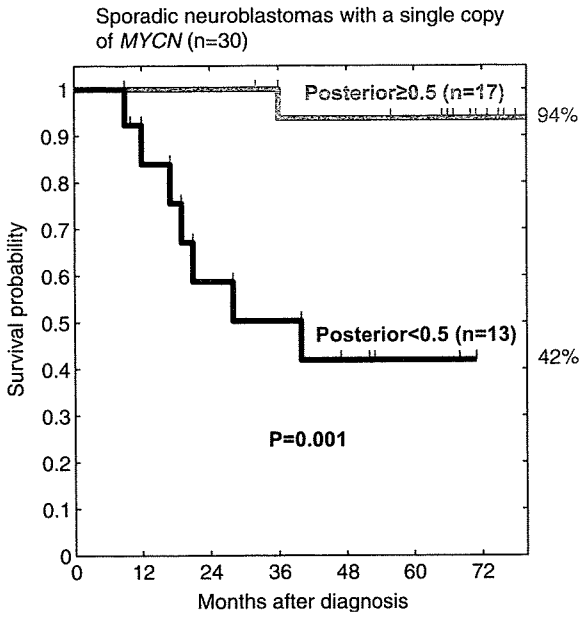


**Figure 4** Kaplan–Meier survival curves of sporadic neuroblastomas with a single copy of *MYCN* according to the molecular signature. Gene-expression profiling segregated patients into the favorable (posterior score⩾0.5) and unfavorable (posterior score<0.5) prognosis groups ($P=0.001$). The posterior score denotes how likely the patient would show good outcome after 5 years (Ohira *et al.*, 2005).

GGW tumors. Since MS did not decrease the incidence of sporadic neuroblastomas (Brodeur *et al.*, 2001; Levy, 2005), GGSs tumors in young and old patients might be derived from different progenitor cells. It is interesting that the clinical outcome is very good for patients with *MYCN*-nonamplified GGSs tumors, whereas it is very bad for patients with GGSa tumors possessing *MYCN* amplification, implying again remarkable impact of *MYCN* amplification on the patient's outcome.

The GGP group is characterized by the presence of 17q gain with other chromosomal abnormalities including *MYCN* amplification, 1p loss and 11q loss. Since this group of tumors shows multiple chromosomal aberrations with partial gains and/or losses, unknown causes to induce genomic instability might have triggered genesis of neuroblastoma in progenitor or stem cells of sympathetic cell lineage (Maris and Matthay, 1999; Nakagawara, 2004). The frequently observed GGP tumors are as follows: GGP1a tumors with both 1p loss and *MYCN* amplification and GGP3s tumors with 11q loss but without *MYCN* amplification. The former may belong to a typical *MYCN*-amplified neuroblastoma (White *et al.*, 1995) with a 5-year cumulative survival rate of 42% in our series, whereas the latter to the so-called intermediate type tumor (Srivatsan *et al.*, 1993; Attiyeh *et al.*, 2005) with the rate of 75%. In GGP tumors, it is obvious that *MYCN* amplification has the most powerful impact on the patient prognosis. Interestingly, among the GGPs tumors lacking *MYCN* amplification, 1p loss and 11q loss seem to similarly affect the prognosis. However, GGP2s tumors with both 1p loss and 11q loss show poorer prognosis in an additive manner. The similar additive effect has also been observed in GGP1a (42%

survival) and GGP2a (0% survival) with *MYCN*-amplified tumors. These suggest that 1p loss and 11q loss may independently affect the outcomes of neuroblastoma. Interestingly, one of the main characteristics of the *MYCN*-amplified tumors found in the long-term survivors is a lack of 11q loss (Supplementary Figure S4), corresponding to the observation that the high percentage of 5-year survival rate is shown in the GGP1a group with 1p loss but without 11q loss.

GGW neuroblastoma has a favorable prognosis, as reported (Vandesompele *et al.*, 1998). Since the pattern of chromosomal aberrations is represented by whole chromosomal gains and/or losses, mitotic dysfunction during the cell division cycle in progenitor or stem cells might have generated neuroblastoma (Maris and Matthay, 1999; Nakagawara, 2004). Interestingly, 1p loss or 11q loss in a minor population of GGWs tumors (GGW1s and GGW3s) seems not to affect the prognosis.

The presence of different patterns of genomic aberrations like GGS, GGP and GGW may reflect differences in stem or progenitor cells targeted to generate different genetic subsets of neuroblastomas. Although carcinogenic events to cause neuroblastomas may occur sequentially (Tonini, 1993), our serial analyses of six paired primary and recurrent tumors interestingly suggest that the major genetic events, for example, *MYCN* amplification, 1p loss, 11q loss and 17q gain, could occur not always in order during tumor progression (Supplementary Table S3).

Thus, the genomic signatures presented here successfully categorized new prognostic subgroups of neuroblastomas. The rather consistent patterns of genomic abnormalities provide reliable information to understanding of the genetic bases which underlie the clinical phenotypes of neuroblastomas with different survival rates. However, the pattern of genomic abnormalities may often lack biological significance affecting the clinical behavior of individual tumors. The gene-expression profile well reflects the biology of individual tumor. Therefore, establishment of the combined system of both genomic and molecular signatures is ideal for predicting the prognosis of individual patients with neuroblastoma. The present study has clearly shown that genomic and molecular signatures are independent prognostic indicators and suggests that an expression microarray could compensate for the relevant lack when used only genomic signature. In conclusion, combined genomic and molecular signatures may be clinically useful for constituting an ideal system to categorize and even individualize each tumor, which may make tailored medicine of neuroblastoma possible.

## Materials and methods

*Patients, tissue specimens and DNA/RNA resources*

Tumor specimens were collected from 236 patients who had undergone biopsy or surgery at various institutions in Japan (see Supplementary Information). They included 112 sporadic and 124 MS-detected neuroblastoma specimens. All tumors were histopathologically diagnosed as neuroblastoma or ganglioneuroblastoma and were staged according to the International Neuroblastoma Staging System (Brodeur *et al.*, 1993). Informed consent was obtained at each institution or hospital. The procedure of this study was approved by the Institutional Review Board of the Chiba Cancer Center (CCC7817). Patients were treated by the standard protocols (Kaneko *et al.*, 2002; Iehara *et al.*, 2006) in Japan between 1995 and 2003. All MS-detected tumors were diagnosed between 6 and 8 months after birth by measuring urinary catecholamine metabolites in Japan (Sawada *et al.*, 1984). Fresh neuroblastoma tissues removed during surgery were stored at −80°C. *MYCN* copy number, *TrkA* mRNA expression and DNA ploidy were measured as reported previously (Islam *et al.*, 2000).

*Microarray-based comparative genomic hybridization*

A chip carrying 2464 BAC clones prepared by ligation-mediated PCR, which covers the whole human genome at roughly 1.2-Mb resolution (Snijders *et al.*, 2001; Albertson *et al.*, 2003), was used. The 500-ng aliquots of tumors and reference DNAs were labeled by random priming with each Cy3-dCTP and Cy5-dCTP (Amersham Pharmacia, Piscataway, NJ, USA). Hybridization was performed as previously reported (Pinkel *et al.*, 1998). UCSF Spot and UCSF Sproc programs to analyse values for spotted clones (Jain *et al.*, 2002) were used. All array-CGH data are available at NCBI Gene Expression Omnibus (GEO, http://www.ncbi.nlm.nih.gov/geo/) with accession number GSE 5784.

*cDNA microarrays*

In-house cDNA microarrays, carrying 5340 cDNAs obtained from the oligo-capping cDNA libraries generated from anonymous neuroblastoma tissues (Ohira *et al.*, 2003, 2005), were used. Preparation of RNA, hybridization, reading of spots and statistical analyses were conducted as reported previously (Ohira *et al.*, 2005). Gene-expression profile data described in this study is available at NCBI GEO with accession number GSE 5779.

*Statistical analysis*

The fluorescence ratio for each array CGH spot was normalized and rescaled into estimated copy number aberrations of each clone according to the comb-fit method (Oba *et al.*, 2006; see also Supplementary Figure S2a). Chromosomal events were detected by locally smoothing variations in copy number aberrations of clones on a chromosome and by applying threshold rules (see Supplementary Figure S2a and Supplementary Information for more detail). The numbers of whole chromosomal events, Nw and of partial chromosomal events, Np, were counted for $22+2$ chromosomes in every specimen, and the scatter plot in the Nw–Np plane exhibited apparent three clusters: whole differential dominant ($Nw > Np$), partial differential dominant ($Nw < Np$) and silent ($Nw \approx 0$, $Np \approx 0$) (Supplementary Figure S2b). To discriminate whole differential dominant from partial differential dominant, we defined a 'global' feature variable $\alpha$ as computationally evaluated as the ratio between Nw and Np; when $\alpha$ was small (large), the sample was likely to be whole (partial) differential dominant (see Supplementary Information for more detail). A differential analysis of gene expression was made using standard *t*-test with the *q*-value analysis (Storey and Tibshirani, 2003) for incorporating a false discovery rate (to deal with multiple statistical tests). A survival analysis was made based on Kaplan–Meier and log-rank tests. Univariate and multivariate analyses were made according to the Cox hazard models.

## Acknowledgements

We thank institutions and hospitals for providing tumor specimens (see Supplementary Information). We also thank Shigeru Sakiyama, Hiroki Nagase, Iwao Nozawa, Tadayuki Koda and technical staff, past and present, at Division of Biochemistry, Chiba Cancer Center Research Institute. We acknowledge Hisamitsu Pharmaceutical Co. Inc., the Ministry of Education, Culture, Sports, Science and Technology of Japan, the Ministry of Health, Labour and Welfare of Japan and the Hamaguchi Foundation for the Advancement of Biochemistry for funding this work.

## References

Albertson DG, Collins C, McCormick F, Gray JW. (2003). Chromosome aberrations in solid tumors. *Nat Genet* **34**: 369–376.

Attiyeh EF, London WB, Mosse YP, Wang Q, Winter C, Khazi D *et al.* (2005). Chromosome 1p and 11q deletions and outcome in neuroblastoma. *N Engl J Med* **353**: 2243–2253.

Bagchi A, Papazoglu C, Wu Y, Capurso D, Brodt M, Francis D *et al.* (2007). CHD5 is a tumor suppressor at human 1p36. *Cell* **128**: 459–475.

Beckwith JB, Perrin EV. (1963). *In situ* neuroblastomas: a contribution to the natural history of neural crest tumors. *Am J Pathol* **43**: 1089–1101.

Brodeur GM. (2003). Neuroblastoma: biological insight into a clinical enigma. *Nat Rev Cancer* **3**: 203–216.

Brodeur GM, Look AT, Shimada H, Hamilton VM, Maris JM, Hann HW *et al.* (2001). Biological aspects of neuroblastomas identified by mass screening in Quebec. *Med Pediatr Oncol* **36**: 157–159.

Brodeur GM, Pritchard J, Berthold F, Carlsen NL, Castel V, Castelberry RP *et al.* (1993). Revisions of the international criteria for neuroblastoma diagnosis, staging, and response to treatment. *J Clin Oncol* **11**: 1466–1477.

Iehara T, Hosoi H, Akazawa K, Matsumoto Y, Yamamoto K, Suita S *et al.* (2006). MYCN gene amplification is a powerful prognostic factor even in infantile neuroblastoma detected by mass screening. *Br J Cancer* **94**: 1510–1515.

Islam A, Kageyama H, Takada N, Kawamoto T, Takayasu H, Isogai E *et al.* (2000). High expression of Survivin, mapped to 17q25, is significantly associated with poor prognostic factors and promotes cell survival in human neuroblastoma. *Oncogene* **19**: 617–623.

Jain AN, Tokuyasu TA, Snijders AM, Segraves R, Albertson DG, Pinkel D. (2002). Fully automatic quantification of microarray image data. *Genome Res* **12**: 325–332.

Kaneko M, Tsuchida Y, Mugishima H, Ohnuma N, Yamamoto K, Kawa K *et al.* (2002). Intensified chemotherapy increases the survival rates in patients with stage 4 neuroblastoma with MYCN amplification. *J Pediatr Hematol Oncol* **24**: 613–621.

Levy IG. (2005). Neuroblastoma, well-designed evaluations, and the optimality of research funding: ask not what your country can do for you. *J Natl Cancer Inst* **97**: 1105–1106.

Look AT, Hayes FA, Nitschke R, McWilliams NB, Green AA. (1984). Cellular DNA content as a predictor of response to chemotherapy in infants with unresectable neuroblastoma. *N Engl J Med* **311**: 231–235.

Maris JM, Matthay KK. (1999). Molecular biology of neuroblastoma. *J Clin Oncol* **17**: 2264–2279.

Nakagawara A. (1998). The NGF story and neuroblastoma. *Med Pediatr Oncol* **31**: 113–115.

Nakagawara A. (2004). Neural crest development and neuroblastoma: the genetic and biological link. *Prog Brain Res* **146**: 233–242.

Nakagawara A, Arima-Nakagawara M, Scavarda NJ, Azar CG, Cantor AB, Brodeur GM. (1993). Association between high levels of expression of the TRK gene and favorable outcome in human neuroblastoma. *N Engl J Med* **328**: 847–854.

Oba S, Tomioka N, Ohira M, Ishii S. (2006). Combfit: a normalization method for array CGH data. *IPSJ Trans Bioinformatics* **47**: 73–82.

Ohira M, Morohashi A, Inuzuka H, Shishikura T, Kawamoto T, Kageyama H *et al.* (2003). Expression profiling and characterization of 4200 genes cloned from primary neuroblastomas: identification of 305 genes differentially expressed between favorable and unfavorable subsets. *Oncogene* **22**: 5525–5536.

Ohira M, Oba S, Nakamura Y, Isogai E, Kaneko S, Nakagawa A *et al.* (2005). Expression profiling using a tumor-specific cDNA microarray predicts the prognosis of intermediate risk neuroblastomas. *Cancer Cell* **7**: 337–350.

Pinkel D, Segraves R, Sudar D, Clark S, Poole I, Kowbel D *et al.* (1998). High resolution analysis of DNA copy number variation using comparative genomic hybridization to microarrays. *Nat Genet* **20**: 207–211.

Sawada T, Hirayama M, Nakata T, Takeda T, Takasugi N, Mori T *et al.* (1984). Mass screening for neuroblastoma in infants in Japan. Interim report of a mass screening study group. *Lancet* **2**: 271–273.

Schwab M, Westermann F, Hero B, Berthold F. (2003). Neuroblastoma: biology and molecular and chromosomal pathology. *Lancet* **4**: 472–480.

Snijders AM, Nowak N, Segraves R, Blackwood S, Brown N, Conroy J *et al.* (2001). Assembly of microarrays for genome-wide measurement of DNA copy number. *Nat Genet* **29**: 263–264.

Srivatsan ES, Ying KL, Seeger RC. (1993). Deletion of chromosome 11 and of 14q sequences in neuroblastoma. *Genes Chromosomes Cancer* **7**: 32–37.

Storey JD, Tibshirani R. (2003). Statistical significance for genome-wide studies. *Proc Natl Acad Sci USA* **100**: 9440–9445.

Tomioka N, Kobayashi H, Kageyama H, Ohira M, Nakamura Y, Sasaki F *et al.* (2003). Chromosomes that show partial loss or gain in near-diploid tumors coincide with chromosomes that show whole loss or gain in near-triploid tumors: evidence suggesting the involvement of the same genes in the tumorigenesis of high- and low-risk neuroblastomas. *Genes Chromosomes Cancer* **36**: 139–150.

Tonini GP. (1993). Neuroblastoma: the result of multistep transformation? *Stem Cells* **11**: 276–282.

Vandesompele J, Van Roy N, Van Gele M, Laureys G, Ambros P, Heimann P *et al.* (1998). Genetic heterogeneity of neuroblastoma studied by comparative genomic hybridization. *Genes Chromosomes Cancer* **23**: 141–152.

Wei JS, Greer BT, Westermann F, Steinberg SM, Son CG, Chen QR *et al.* (2004). Prediction of clinical outcome using gene expression profiling and artificial neural networks for patients with neuroblastoma. *Cancer Res* **64**: 6883–6891.

White PS, Maris JM, Beltinger C, Sulman E, Marshall HN, Fujimori M *et al.* (1995). A region of consistent deletion in neuroblastoma maps within human chromosome 1p36.2–36.3. *Proc Natl Acad Sci USA* **92**: 5520–5524.

Woods WG, Gao RN, Shuster JJ, Robison LL, Bernstein M, Weitzman S *et al.* (2002). Screening of infants and mortality due to neuroblastoma. *N Engl J Med* **346**: 1041–1046.

Supplementary Information accompanies the paper on the Oncogene web site (http://www.nature.com/onc).

Vol 455|16 October 2008|doi:10.1038/nature07399

nature

LETTERS

# Oncogenic mutations of ALK kinase in neuroblastoma

Yuyan Chen[1,2,3]*, Junko Takita[1,2,3]*, Young Lim Choi[4]*, Motohiro Kato[1,3], Miki Ohira[5], Masashi Sanada[2,3,6], Lili Wang[2,3,6], Manabu Soda[4], Akira Kikuchi[7], Takashi Igarashi[1], Akira Nakagawara[5], Yasuhide Hayashi[8], Hiroyuki Mano[4,6] & Seishi Ogawa[2,3,6]

**Neuroblastoma in advanced stages is one of the most intractable paediatric cancers, even with recent therapeutic advances[1]. Neuroblastoma harbours a variety of genetic changes, including a high frequency of *MYCN* amplification, loss of heterozygosity at 1p36 and 11q, and gain of genetic material from 17q, all of which have been implicated in the pathogenesis of neuroblastoma[2–5]. However, the scarcity of reliable molecular targets has hampered the development of effective therapeutic agents targeting neuroblastoma. Here we show that the anaplastic lymphoma kinase (ALK), originally identified as a fusion kinase in a subtype of non-Hodgkin's lymphoma (NPM–ALK)[6–8] and more recently in adenocarcinoma of lung (EML4–ALK)[9,10], is also a frequent target of genetic alteration in advanced neuroblastoma. According to our genome-wide scans of genetic lesions in 215 primary neuroblastoma samples using high-density single-nucleotide polymorphism genotyping microarrays[11–14], the *ALK* locus, centromeric to the *MYCN* locus, was identified as a recurrent target of copy number gain and gene amplification. Furthermore, DNA sequencing of *ALK* revealed eight novel missense mutations in 13 out of 215 (6.1%) fresh tumours and 8 out of 24 (33%) neuroblastoma-derived cell lines. All but one mutation in the primary samples (12 out of 13) were found in stages 3–4 of the disease and were harboured in the kinase domain. The mutated kinases were autophosphorylated and displayed increased kinase activity compared with the wild-type kinase. They were able to transform NIH3T3 fibroblasts as shown by their colony formation ability in soft agar and their capacity to form tumours in nude mice. Furthermore, we demonstrate that downregulation of *ALK* through RNA interference suppresses proliferation of neuroblastoma cells harbouring mutated *ALK*. We anticipate that our findings will provide new insights into the pathogenesis of advanced neuroblastoma and that *ALK*-specific kinase inhibitors might improve its clinical outcome.**

To identify oncogenic lesions in neuroblastoma, we performed a genome-wide analysis of primary tumour samples obtained from 215 neuroblastoma patients using high-density single-nucleotide polymorphism (SNP) arrays (Affymetrix GeneChip 250K *Nsp*I) (Supplementary Table 1). Twenty-four neuroblastoma-derived cell lines were also analysed (Supplementary Table 2). Interrogating over 250,000 SNP sites, this platform permits the identification of copy number changes at an average resolution of less than 12 kilobases (kb)[13,14].

Analysis of this large number of samples, consisting of varying disease stages, permitted us to obtain a comprehensive registry of genomic lesions in neuroblastoma (Supplementary Figs 1 and 2). A gain of chromosomes, often triploid or hyperploid (defined by mean copy number of >2.5), was a predominant feature of neuroblastoma genomes in the lower stages. Ploidy generally correlated with the clinical stage, where non-hyperploid cases were significantly associated with stage 4 disease ($P = 4.13 \times 10^{-5}$, trend test) (Supplementary Fig. 3 and Supplementary Table 3). 17q gains, frequently in multiple copies (3≤ copy number <5), were a hallmark of the neuroblastoma genome[4] and were found in most neuroblastoma cases. Copy number gains tended to spare chromosomes 3, 4, 10, 14 and 19 (Supplementary Figs 2 and 3). Notably, these chromosomes often had copy number losses including 1p (22.8%), 3p (8.8%), 4p (5.1%), 6q (7.0%), 10q (9.8%), 11q (19.5%), 14q (3.7%), 19p (7.4%) and 19q (5.1%), implicating the pathogenic role of 'relative' gene dosages.

After excluding known copy number variations, we identified a total of 28 loci undergoing high-grade amplifications (copy number ≥5) (Supplementary Table 4). These lesions fell into relatively small genomic segments, having a mean size of 361 kb, which accelerated the identification of gene targets in these regions (Supplementary Table 4 and Supplementary Fig. 4). The candidate gene targets included *TERT* (5p15.33), *HDAC3* (5q31.3), *IGF2* (11p15.1), *MYEOV* (11q13.3), *FGF7* (15q21.1) and *CDH13* (16q23.3). However, many of them were not recurrent but found only in a single case. Although the recurrent lesions were mostly explained by the amplification of *MYCN* at 2p24, as found in 50 out of 215 (23%) of the primary cases, we identified another peak of recurrent amplification at 2p23 (Fig. 1a), which consisted of amplicons in five primary cases and in one neuroblastoma-derived cell line, NB-1 (Supplementary Fig. 5). This peak was located at the centromeric margin of the common copy number gains in chromosome 2p, which was created by copy number gains in 109 samples mostly from non-hyperploid stage 4 cases. The minimum overlapping amplification was defined by the amplicons found in the NB-1 cell line (Supplementary Fig. 5) and contained a single gene, the anaplastic lymphoma kinase (*ALK*), which has previously been reported to be overexpressed in neuroblastoma cases[15]. Although five of the six samples showing *ALK* amplification also had *MYCN* amplification, one primary case (NT056) lacked a *MYCN* peak and the amplification was confined to the *ALK*-containing locus. In interphase fluorescent *in situ* hybridization (FISH) analysis of NB-1, *MYCN* and *ALK* loci were amplified in separate amplicons (Fig. 1b), indicating that the 2p23 amplicons containing *ALK* were unlikely to represent merely 'passenger' events of *MYCN* amplification but actively contributed to the pathogenesis of neuroblastoma.

Because an oncogene can be activated by gene amplification and/or mutation, to search for possible mutations we performed DNA heteroduplex formation analysis[16] and genomic DNA sequencing for the exons 20 to 28 of *ALK*, which encompass the juxtamembrane and kinase domains (Supplementary Table 5). In total, we identified eight nucleotide changes in 21 neuroblastoma samples, 13 out of 215

[1]Department of Pediatrics, [2]Cell Therapy and Transplantation Medicine, [3]Cancer Genomics Project, Graduate School of Medicine, The University of Tokyo, Tokyo 113-8655, Japan. [4]Division of Functional Genomics, Jichi Medical University, Toguchi 329-0498, Japan. [5]Division of Biochemistry, Chiba Cancer Center Research Institute, Chiba 260-8717, Japan. [6]Core Research for Evolutional Science and Technology, Japan Science and Technology Agency, Saitama, 332-0012, Japan. [7]Division of Hematology/Oncology, Saitama Children's Medical Center, Saitama 339-8551, Japan. [8]Gunma Children's Medical Center, Shibukawa 377-8577, Japan.
*These authors contributed equally to this work.

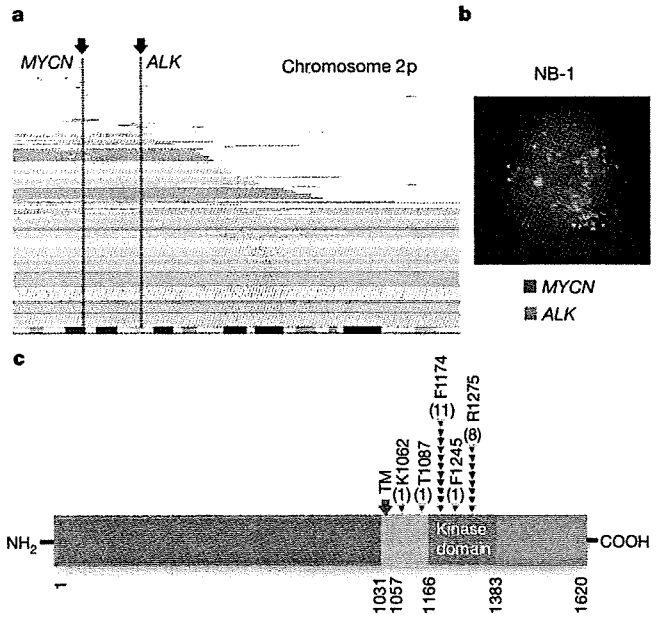


**Figure 1 | Common 2p gains/amplifications and *ALK* mutations in neuroblastoma samples.** **a**, Recurrent copy number gains on the 2p arm. High-grade amplifications are shown by light-red horizontal lines, whereas simple gains are shown by dark-red lines. Two common peaks of copy number gains and amplifications in the *MYCN* and *ALK* loci are indicated by arrows. The cytobands in 2p are shown at the bottom. **b**, Interphase FISH analysis of NB-1 showing high-grade amplification of *MYCN* (red) and *ALK* loci (green). The amplified *MYCN* locus appears as a single large signal. **c**, Distribution of the eight *ALK* mutations found in 21 neuroblastoma samples. The positions of the mutated amino acids are indicated by black (primary samples) and red (cell lines) arrowheads. The number of mutations at each site is shown at the top of the arrowheads. TM, transmembrane.

(6.1%) primary samples and 8 out of 24 (33%) cell lines, which resulted in seven types of amino acid substitutions at five different positions (Table 1 and Supplementary Fig. 6). They were not found in either the genomic DNA collected from 50 healthy volunteers or in the SNP databases at the time of preparing this manuscript. In fact, somatic origins of missense changes were confirmed in 9 out of 13 primary cases, for which DNA was obtained from the peripheral blood or the tumour-free bone marrow specimens (Supplementary Fig. 6). On the other hand, T1087I (ACC>ATC), found in case NT126, had a germline origin and thus it could not be determined whether the T1087I change was a rare non-functional polymorphism or represented a pathogenic germline mutation. For other changes found in three primary cases (NT128, NT217 and NT218) and cell lines, normal DNA was not available but they were likely to represent oncogenic mutations because they were identical to common somatic changes (F1174L or R1275Q) or shown to have oncogenic potential in functional assays (K1062M).

Most mutations occurred within the kinase domain (20 out of 22 or 91%), which clearly showed two mutation hotspots at F1174 and R1275 (Fig. 1c). A neuroblastoma-derived cell line, SJNB-2, had a homozygous *ALK* mutation of R1275Q, which was probably due to uniparental disomy of chromosome 2 (Supplementary Fig. 7a). Another case (NT074) harboured two different mutations, F1174L and R1275Q, but it remains to be determined whether both are on the same allele. ALK mutations within the kinase domain occurred at amino acid positions that are highly conserved across species and during molecular evolution (Supplementary Figs 8 and 9). According to the conserved structure of other insulin receptor kinases we predicted that F1174 is located at the end of the Cα1 helix, whereas the other two are on the two β-sheets: before the catalytic loop (β6, F1245) and within the activation loop (β9, R1275) (Supplementary Fig. 7b, c)[17]. Thus, conformational changes due to amino acid substitutions at these positions might be responsible for the aberrant activity of the mutant kinases.

**Table 1 | *ALK* mutations/amplifications in neuroblastoma samples**

| Sample | Age (months) | Stage | *MYCN** | Clinical outcome | Mutations/ amplifications | Nucleotide substitution | Origin of mutations |
|---|---|---|---|---|---|---|---|
| NT126 | 99 | 4 | − | Dead | T1087I | ACC>ATC | Germ line |
| NT218 | 8 | 1 | − | Alive | F1174L | TTC>TTG | ND |
| NT074 | 34 | 3 | + | Dead | F1174L | TTC>TTA | Somatic |
| | | | | | R1275Q | CGA>CAA | |
| NT160 | 12 | 4 | + | Dead | F1174L | TTC>TTA | Somatic |
| NT217 | 24 | 4 | + | Dead | F1174L | TTC>TTA | ND |
| NT190 | 48 | 4 | + | Alive | F1174L | TTC>TTA | Somatic |
| NT060 | 163 | 3 | − | Alive | F1174C | TTC>TGC | Somatic |
| NT162 | 28 | 4 | + | Dead | F1174V | TTC>GTC | Somatic |
| NT195 | 24 | 4 | + | Alive | F1245L | TTC>TTG | Somatic |
| NT055 | 6 | 3 | − | Alive | R1275Q | CGA>CAA | Somatic |
| NT128 | 8 | 4 | − | Dead | R1275Q | CGA>CAA | ND |
| NT164 | 54 | 4 | + | Dead | R1275Q | CGA>CAA | Somatic |
| NT200 | 133 | 4 | − | Dead | R1275Q | CGA>CAA | Somatic |
| SCMC-N5† | - | - | + | - | K1062M | AAG>ATG | ND |
| SJNB-4† | - | - | + | - | F1174L | TTC>TTA | ND |
| LAN-1† | - | - | + | - | F1174L | TTC>TTA | ND |
| SCMC-N2† | - | - | + | - | F1174L | TTC>TTA | ND |
| SK-N-SH† | - | - | − | - | F1174L | TTC>TTA | ND |
| SJNB-2†‡ | - | - | + | - | R1275Q | CGA>CAA | ND |
| LAN-5† | - | - | + | - | R1275Q | CGA>CAA | ND |
| TGW† | - | - | + | - | R1275Q | CGA>CAA | ND |
| NT204 | 12 | 1 | + | Alive | Amplification | - | - |
| NT056 | 11 | 3 | − | Dead | Amplification | - | - |
| NT071 | 36 | 3 | + | Alive | Amplification | - | - |
| NT165 | 19 | 4 | + | Dead | Amplification | - | - |
| NT169 | 7 | 4 | + | Dead | Amplification | - | - |
| NB-1† | - | - | + | - | Amplification | - | - |

ND, not determined.
*Presence (+) or absence (−) of *MYCN* amplification in FISH analysis. All cases where there was an absence of *MYCN* amplification (−) were also checked for possible *MYCN* mutations by sequencing of all *MYCN* exons, but no *MYCN* mutations were identified.
† Cell lines.
‡ Homozygous mutation.

*ALK* mutation highly correlated with *MYCN* amplification ($P = 1.55 \times 10^{-4}$, Fisher's exact test; Supplementary Table 6) where 14 out of 21 mutations coexisted with *MYCN* amplification. Regardless of the status of *MYCN* amplification, 12 of the 13 mutations were found in patients with advanced stage neuroblastoma (Table 1). However, whereas *MYCN* amplification and stage 4 were significant risk factors for poor survival, the mutation/amplification status of *ALK* was not likely to have a major impact on survival (Supplementary Fig. 10 and Supplementary Table 7), although the statistical power of the current analysis was largely limited in order to detect a marginal hazard.

To evaluate the impact of ALK mutations on kinase activity, we generated Flag-tagged constructs of ALK and its mutants, F1174L and K1062M, which were stably expressed in NIH3T3 cells, and examined their phosphorylation status and *in vitro* kinase activity. The ALK mutants stably expressed in NIH3T3 cells were phosphorylated according to western blot analysis using an antibody specific for phosphorylated ALK (anti-pY1604) and a PY20 blot after anti-Flag immunoprecipitation of the mutant kinases (Fig. 2a), whereas the wild-type kinase was not phosphorylated. The immunoprecipitated ALK mutants also showed increased tyrosine kinase activity *in vitro* when compared with wild-type ALK. This was shown using both a universal substrate for tyrosine kinase (poly-GluTyr) and the synthetic YFF peptide[18], which was derived from a sequence of the activation loop of *ALK* (Fig. 2b, c). In accordance with these findings, downstream molecules of ALK signalling including AKT, STAT3 and ERK[15] were activated in cells expressing mutant ALK, as shown by their increased phosphorylation (Fig. 2d).

Next, we investigated the oncogenic potential of these mutants. NIH3T3 cells stably expressing mutant kinases showed increased colony formation in soft agar compared with the wild-type protein (Fig. 3a and Supplementary Fig. 11). The tumorigenicity of these ALK mutants was further assayed by injecting $1.0 \times 10^7$ NIH3T3 cells into nude mice. The NIH3T3 cells transfected with the ALK mutants showed focus-forming capacity and developed subcutaneous tumours (6 out of 6 inoculations) 21 days after inoculation, whereas the mock and wild-type ALK-transfected cells did not (0 out of 6 inoculations) (Fig. 3b, c). Finally, we examined the effect of ALK inhibition on the proliferation of neuroblastoma-derived cell lines. RNA interference (RNAi)-mediated *ALK* knockdown resulted in reduced cell proliferation of SK-N-SH cells harbouring the F1174L mutation, but the effects were less clear in wild-type ALK-expressing LAN-2 cells (Fig. 3d, e). Of particular interest is a recent report that 5 out of 17 neuroblastoma-derived cell lines, including SK-N-SH and NB-1, frequently showed high sensitivity to the specific ALK inhibitor TAE684 (ref. 19).

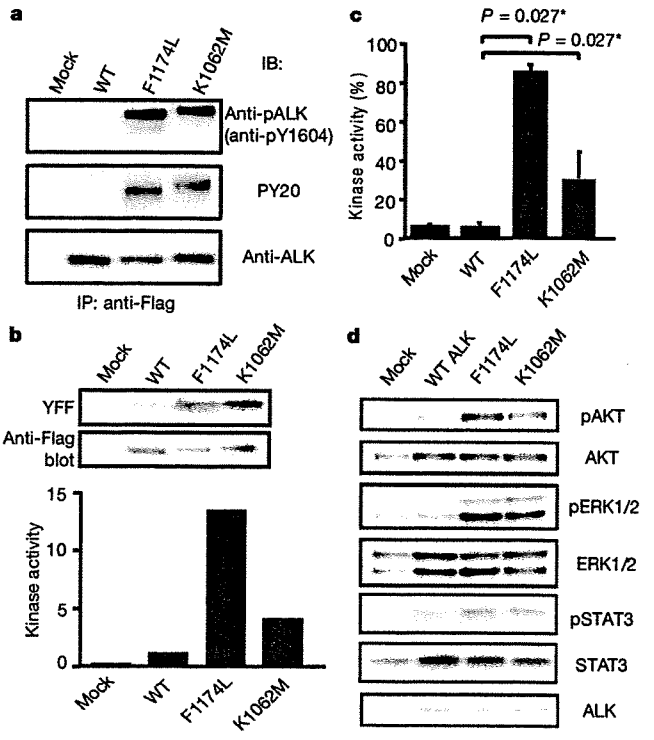


**Figure 2 | Kinase activity of ALK mutants and their downstream signalling.** **a**, Stably expressed ALK and its mutants (F1174L and K1062M) were immunoprecipitated with an anti-Flag antibody and subjected to western blot analysis with anti-pY1604 (upper panel) or PY20 (middle panel). An anti-ALK blot of precipitated kinases is also displayed (bottom panel). **b**, *In vitro* kinase assay for wild-type ALK kinase and its mutants using the synthetic YFF peptide as a substrate, where kinase activity is expressed as relative values to that for wild-type kinase based on the densities in the autoradiogram. **c**, Kinase activity was also assayed for the poly-GluTyr peptide. Significantly different measurements are indicated by asterisks with *P* values. Bars show mean (±s.d.) in three independent experiments. **d**, Western blot analyses of NIH3T3 cells expressing wild-type and mutant ALK for phosphorylated forms of AKT (pAKT), ERK (pERK1/2) and STAT3 (pSTAT3). The total amount of each molecule is also displayed (AKT, ERK1/2, and STAT3) together with an anti-ALK blot (ALK).

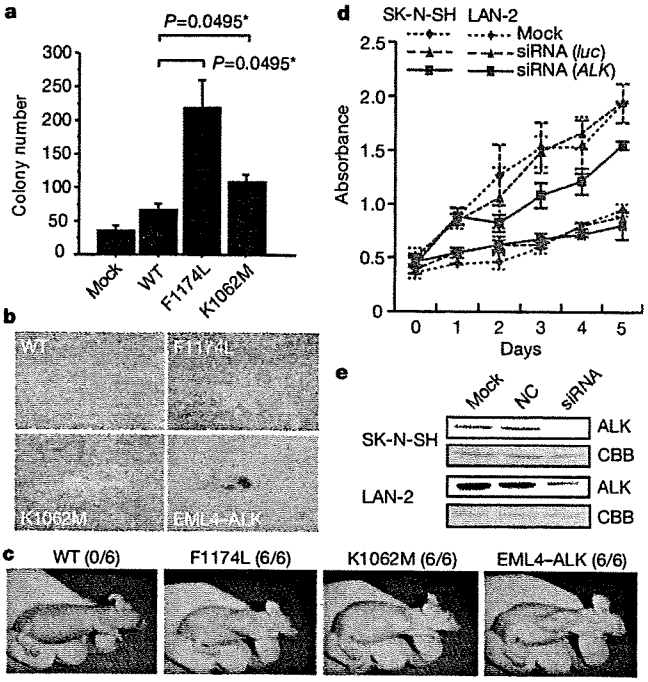


**Figure 3 | Oncogenic role of ALK mutations.** **a**, Colony assays for NIH3T3 cells stably expressing wild-type as well as mutant ALK (F1174L and K1062M). The average numbers of colonies in triplicate experiments are plotted and standard deviation is indicated. Results showing statistically significant differences as compared with experiments using wild-type ALK are indicated by asterisks with *P* values. **b**, **c**, NIH3T3 cells were transfected with wild-type and mutant ALK (F1174L, K1062M and EML4–ALK) and subjected to a focus forming assay (**b**) as well as an *in vivo* tumorigenicity assay in nude mice (**c**). **d**, Effect of RNAi-mediated ALK knockdown on cell proliferation in neuroblastoma cell lines expressing either the F1174L mutant (SK-N-SH) or wild-type ALK (LAN-2). Cell growth was measured using the Cell Counting Kit-8 after knockdown experiments using *ALK*-specific siRNAs (siRNA *ALK*), control siRNAs (siRNA *luc*), or mock experiments, where absorbance was measured in triplicate and averaged for each assay. To draw growth curves, the mean ± s.d. of the averaged absorbance in three independent knockdown experiments is plotted. **e**, Successful knockdown of ALK protein was confirmed by anti-ALK blots (ALK) using Coomassie brilliant blue G-250 (CBB) staining as loading controls. NC, control siRNA; siRNA, *ALK* siRNA.

Through the genome-wide analysis of genetic lesions in neuroblastoma, we identified novel oncogenic *ALK* mutations in advanced neuroblastoma. Combined with the cases having a high-grade amplification of the *ALK* gene, aberrant ALK signalling was likely to be involved in 11% (16 out of 151) of the advanced neuroblastoma cases. Because ALK kinase has been shown to be deregulated only in the form of a fusion kinase in human cancers, including lymphoma and lung cancer, the identification of oncogenic mutations in *ALK* not only increases our understanding of the molecular pathogenesis of advanced neuroblastoma, but also adds a new paradigm to the concept of 'ALK-positive human cancers' in that the mutated *ALK* kinases themselves might participate in human cancers. Our results again highlight the power of genome-wide studies to clarify the genetic lesions in human cancers[20–22]. Given that *ALK* mutations are preferentially involved in advanced neuroblastoma cases having a poor prognosis, our findings implicate that *ALK* inhibitors may improve the clinical outcome of children suffering from intractable neuroblastoma.

## METHODS SUMMARY

Genomic DNA from 215 patients with primary neuroblastoma and 24 neuroblastoma-derived cell lines was analysed on GeneChip SNP genotyping microarrays (Affymetrix GeneChip 250K *Nsp*I). After appropriate normalization of mean array intensities, signal ratios were calculated between tumours and anonymous normal references in an allele-specific manner, and allele-specific copy numbers were inferred from the observed signal ratios based on the hidden Markov model using CNAG/AsCNAR software[13,14]. *ALK* mutations were examined by DNA heteroduplex analysis and/or genomic DNA sequencing[16]. Full-length cDNAs for mutant *ALK* were isolated by high-fidelity PCR and inserted into pcDNA3 and pMXS. The expression plasmids were transfected into NIH3T3 cells using Effectene Transfection Reagent (Qiagen) or by calcium phosphate methods[9]. Western blot analysis of mutant ALK kinases, *in vitro* kinase assays, and tumour formation assays in nude mice were performed as previously described[9]. This study was approved by the ethics boards of the University of Tokyo and of the Chiba Cancer Center Research Institute.

**Full Methods** and any associated references are available in the online version of the paper at www.nature.com/nature.

**Received 3 June; accepted 28 August 2008.**


1. Maris, J. M., Hogarty, M. D., Bagatell, R. & Cohn, S. L. Neuroblastoma. *Lancet* 369, 2106–2120 (2007).
2. Maris, J. M. *et al.* Loss of heterozygosity at 1p36 independently predicts for disease progression but not decreased overall survival probability in neuroblastoma patients: a Children's Cancer Group study. *J. Clin. Oncol.* 18, 1888–1899 (2000).
3. Attiyeh, E. F. *et al.* Chromosome 1p and 11q deletions and outcome in neuroblastoma. *N. Engl. J. Med.* 353, 2243–2253 (2005).
4. Bown, N. *et al.* Gain of chromosome arm 17q and adverse outcome in patients with neuroblastoma. *N. Engl. J. Med.* 340, 1954–1961 (1999).
5. Brodeur, G. M., Seeger, R. C., Schwab, M., Varmus, H. E. & Bishop, J. M. Amplification of N-myc in untreated human neuroblastomas correlates with advanced disease stage. *Science* 224, 1121–1124 (1984).
6. Shiota, M. *et al.* Anaplastic large cell lymphomas expressing the novel chimeric protein p80NPM/ALK: a distinct clinicopathologic entity. *Blood* 86, 1954–1960 (1995).
7. Morris, S. W. *et al.* Fusion of a kinase gene, ALK, to a nucleolar protein gene, NPM, in non-Hodgkin's lymphoma. *Science* 263, 1281–1284 (1994).
8. Fujimoto, J. *et al.* Characterization of the transforming activity of p80, a hyperphosphorylated protein in a Ki-1 lymphoma cell line with chromosomal translocation t(2;5). *Proc. Natl Acad. Sci. USA* 93, 4181–4186 (1996).
9. Soda, M. *et al.* Identification of the transforming *EML4–ALK* fusion gene in non-small-cell lung cancer. *Nature* 448, 561–566 (2007).
10. Rikova, K. *et al.* Global survey of phosphotyrosine signaling identifies oncogenic kinases in lung cancer. *Cell* 131, 1190–1203 (2007).
11. Kennedy, G. C. *et al.* Large-scale genotyping of complex DNA. *Nature Biotechnol.* 21, 1233–1237 (2003).
12. Matsuzaki, H. *et al.* Genotyping over 100,000 SNPs on a pair of oligonucleotide arrays. *Nature Methods* 1, 109–111 (2004).
13. Nannya, Y. *et al.* A robust algorithm for copy number detection using high-density oligonucleotide single nucleotide polymorphism genotyping arrays. *Cancer Res.* 65, 6071–6079 (2005).
14. Yamamoto, G. *et al.* Highly sensitive method for genomewide detection of allelic composition in nonpaired, primary tumor specimens by use of affymetrix single-nucleotide-polymorphism genotyping microarrays. *Am. J. Hum. Genet.* 81, 114–126 (2007).
15. Osajima-Hakomori, Y. *et al.* Biological role of anaplastic lymphoma kinase in neuroblastoma. *Am. J. Pathol.* 167, 213–222 (2005).
16. Donohoe, E. Denaturing high-performance liquid chromatography using the WAVE DNA fragment analysis system. *Methods Mol. Med.* 108, 173–187 (2005).
17. Hu, J., Liu, J., Ghirlando, R., Saltiel, A. R. & Hubbard, S. R. Structural basis for recruitment of the adaptor protein APS to the activated insulin receptor. *Mol. Cell* 12, 1379–1389 (2003).
18. Donella-Deana, A. *et al.* Unique substrate specificity of anaplastic lymphoma kinase (ALK): development of phosphoacceptor peptides for the assay of ALK activity. *Biochemistry* 44, 8533–8542 (2005).
19. McDermott, U. *et al.* Genomic alterations of anaplastic lymphoma kinase may sensitize tumors to anaplastic lymphoma kinase inhibitors. *Cancer Res.* 68, 3389–3395 (2008).
20. Garraway, L. A. *et al.* Integrative genomic analyses identify MITF as a lineage survival oncogene amplified in malignant melanoma. *Nature* 436, 117–122 (2005).
21. Mullighan, C. G. *et al.* Genome-wide analysis of genetic alterations in acute lymphoblastic leukaemia. *Nature* 446, 758–764 (2007).
22. Kawamata, N. *et al.* Molecular allelokaryotyping of pediatric acute lymphoblastic leukemias by high-resolution single nucleotide polymorphism oligonucleotide genomic microarray. *Blood* 111, 776–784 (2008).


**Supplementary Information** is linked to the online version of the paper at www.nature.com/nature.

**Acknowledgements** We thank H. P. Koeffler for critically reading and editing the manuscript. We also thank M. Matsumura, Y. Ogino, S. Ichimura, S. Sohma, E. Matsui, Y. Yin, N. Hoshino and Y. Nakamura for their technical assistance. This work was supported by the Core Research for Evolutional Science and Technology, Japan Science and Technology Agency and by a Grant-in-Aid from the Ministry of Health, Labor and Welfare of Japan for the third-term Comprehensive 10-year Strategy for Cancer Control.

**Author Contributions** Y.C., Y.L.C. and J.T. contributed equally to this work. M.K. and M.Sa. performed microarray experiments and subsequent data analyses. Y.C. and J.T. performed mutation analysis of *ALK*. Y.C., Y.L.C., J.T., M.So., L.W. and H.M. conducted functional assays of mutant ALK. A.N., M.O., T.I., A.K. and Y.H. prepared tumour specimens and were involved in statistical analysis. A.N., Y.H., H.M., J.T. and S.O. designed the overall study, and S.O. and J.T. wrote the manuscript. All authors discussed the results and commented on the manuscript.

**Author Information** The nucleotide sequences of *ALK* mutations detected in this study have been deposited in GenBank under the accession numbers EU788003 (K1062M), EU788004 (T1087I), EU788005 (F1174L; TTC/TTA), EU788006 (F1174L; TTC/TTG), EU788007 (F1174C), EU788008 (F1174V), EU788009 (F1245L) and EU788010 (R1275Q). The copy number data as well as the raw microarray data will be accessible from http://www.ncbi.nlm.nih.gov/geo/ with the accession number GSE12494. Reprints and permissions information is available at www.nature.com/reprints. Correspondence and requests for materials should be addressed to S.O. (sogawa-tky@umin.net) or Y.H. (hayashiy-tky@umin.ac.jp).

## METHODS

**Specimens.** Primary neuroblastoma specimens were obtained during surgery or biopsy from patients who were diagnosed with neuroblastoma and admitted to a number of hospitals in Japan. In total, 215 primary neuroblastoma specimens were subjected to SNP array analysis after informed consent was obtained from the parents of each patient. The patients were staged according to the International Neuroblastoma Staging System[23]. The clinicopathological findings are summarized in Supplementary Table 1. Twenty-four neuroblastoma-derived cell lines were also analysed by SNP array analysis (Supplementary Table 2). The SCMC-N2, SCMC-N4 and SCMC-N5 cell lines were established in our laboratory[24,25]. The SJNB series of cells and the UTP-N-1[26] cell line were gifts from A. T. Look and A. Inoue, respectively. The other cell lines used were obtained from the Japanese Cancer Resource Cell Bank (http://cellbank.nibio.go.jp/).

**Microarray analysis.** High molecular mass DNA was isolated from tumour specimens as well as from the peripheral blood or the bone marrow as described previously[24]. The DNA was subjected to SNP array analysis using Affymetrix GeneChip Mapping 50K and/or 250K arrays (Affymetrix) according to the manufacturer's suggested protocol. The scanned array images were processed with Gene Chip Operation software (GCOS)[13], followed by SNP calls using GTYE. Genome-wide copy number measurements and loss of heterozygosity detection were performed using CNAG/AsCNAR algorithms[14], which enabled an accurate determination of allele-specific copy numbers.

**Confirmation of SNP array data.** FISH and/or genomic PCR analysis confirmed the results of SNP array analyses as described previously[13]. PCR primer sets were designed to amplify several adjacent fragments inside and outside of the homozygously deleted regions in tumour samples.

**Mutation analysis.** Mutations in the *ALK* gene were examined in 239 neuroblastoma samples, including 24 cell lines, by denaturing high-performance liquid chromatography (DHPLC) using the WAVE system (Model 4500; Transgenomic) according to the manufacturer's suggested protocol[16]. The samples showing abnormal conformations were subjected to direct sequencing analysis using an ABI PRISM 3100 Genetic Analyser (Applied Biosystems). Using direct sequencing, mutation analysis of *MYCN* was also performed in seven cases with *ALK* alterations but not *MYCN* amplification. The primer sets used in this study are listed in Supplementary Table 5.

**Transforming potential of *ALK* mutants.** Total RNA was extracted from SJNB-1 (wild type), SCMC-N2 (F1174L) and SCMC-N5 (K1062M) cells as described previously[26]. First-strand cDNA was synthesized from RNA using Transcriptor Reverse Transcriptase and an oligo (dT) primer (Roche Applied Science). The resulting cDNA was then amplified by PCR using the KOD-Plus-Ver.2 DNA polymerase (Toyobo) and the primers sense 5′-TCAGAAGCTTTACCAAGGACTGTTCAGAGC-3′ and antisense 5′-AATTGCGGCCGCTACTTGTCATCGTCGTCCTTGTAGTCGGGCCCAGGCTG GTTCATGC-3′, thereby introducing a HindIII site at the 5′ terminus and a NotI site and a Flag sequence at the 3′ terminus. The HindIII–NotI fragments of *ALK* cDNA were subcloned into pcDNA3 to generate expression plasmids. After resequencing to confirm that they had no other mutations, the *ALK* plasmids were used for transfection into NIH3T3 cells using Effectene Transfection Reagent (Qiagen) according to the suggested manufacturer's protocol. The transfected NIH3T3 cells were selected in 800 $\mu g\,ml^{-1}$ G418 for 2 weeks to obtain stably expressing clones.

To evaluate the phosphorylation status of ALK mutants, the cell lysates of stable clones were immunoprecipitated with antibodies to Flag (Sigma) and the resulting precipitates were subjected to western blot analysis with the antibody specific to pTyr 1604 (Cell Signaling Technology) of ALK and the generic anti-phosphotyrosine antibody (PY20). The *in vitro* kinase activity of ALK mutants was measured using a non-radioactive isotope solid-phase enzyme-linked immunosorbent assay using the Universal Tyrosine Kinase Assay kit (Takara) according to the manufacturer's suggested protocol. We also performed the *in vitro* kinase assay with the synthetic YFF peptide (Operon Biotechnologies) as described previously[18]. For anchorage-independent growth analysis, $1 \times 10^3$ stably transfected NIH3T3 cells were mixed in 0.3% agarose with 10% FBS-DMEM and plated on 0.6% agarose-coated 35-mm dishes. After culture for 28 days, the colonies of >0.1 mm in diameter were counted. The quantification of the colonies was from three independent experiments. To investigate the downstream signalling of ALK, western blot analysis was performed using the anti-ERK1/2, anti-phospho-ERK1/2, anti-AKT, anti-phospho-AKT, anti-STAT3 and anti-phospho-STAT3 antibodies (Cell Signaling Technology)[15].

The cDNA mutant of *ALK* was also inserted into the pMXS plasmid and the constructs were introduced into NIH3T3 cells by the calcium phosphate method as described previously[9]. The cells were then either cultured for 21 days or injected subcutaneously at six sites in three nude mice.

**Inhibition of ALK through RNAi-mediated knockdown.** To suppress the expression of the ALK protein, two different pairs of *ALK* siRNAs (*ALK* siRNA1 and *ALK* siRNA2) were obtained (Qiagen)[15]. The sequences were 5′-GAGUCUGGCAGUUGACUUCdTdT-3′ for *ALK* siRNA1 and 5′-GCUCCGGCGUGCCAAGCAGdTdT-3′ for *ALK* siRNA2. A siRNA, targeting a sequence in firefly (*Photinus pyralis*) luciferase mRNA (*luc* siRNA), was used as a negative control (Qiagen)[15]. The sequences of *luc* siRNA were as follow: sense 5′-CGUACGCGGAAUACUUCGAdTdT-3′ and antisense 5′-UCGAAGUAUUCCGCGUACGdTdT-3′. Gene knockdown was achieved in SK-N-SH and LAN-2 cells using HiPerFect transfection reagent following the manufacturer's suggested instructions (Qiagen). To assess the effect of ALK knockdown on cell growth, these cells were seeded in 96-well plates at a concentration of $8.0 \times 10^3$ cells per well 24 h before transfection and assayed using the Cell Counting Kit-8 (Wako).

**Statistical analysis.** The significance of the correlation between *MYCN* amplification and *ALK* mutation was tested according to the conventional $2 \times 2$ contingency table using Fisher's exact test. The significance of the differences in kinase activity between wild-type and mutant ALK kinases was examined by the Mann–Whitney *U*-test based on the measured percentage activity of kinases in the precipitates of the corresponding samples. The significance of the differences in colony formation between wild-type and mutant ALK kinases was also examined by the Mann–Whitney *U*-test. The size of the hazards from possible risk factors, including International Neuroblastoma Staging System stages, *MYCN* status and *ALK* mutation/amplification were estimated by Cox regression analysis assuming a proportional hazard model using Stata software. Correlation between ploidy and clinical stage was tested by nptrend test.


23. Smith, E. I., Haase, G. M., Seeger, R. C. & Brodeur, G. M. A surgical perspective on the current staging in neuroblastoma—the International Neuroblastoma Staging System proposal. *J. Pediatr. Surg.* 24, 386–390 (1989).
24. Takita, J. *et al.* Allelotype of neuroblastoma. *Oncogene* 11, 1829–1834 (1995).
25. Takita, J. *et al.* Absent or reduced expression of the caspase 8 gene occurs frequently in neuroblastoma, but not commonly in Ewing sarcoma or rhabdomyosarcoma. *Med. Pediatr. Oncol.* 35, 541–543 (2000).
26. Takita, J. *et al.* Allelic imbalance on chromosome 2q and alterations of the caspase 8 gene in neuroblastoma. *Oncogene* 20, 4424–4432 (2001).

*Pediatric Hematology and Oncology*, 25:439–450, 2008

ISSN: 0888-0018 print / 1521-0669 online
DOI: 10.1080/08880010802104601

informa
healthcare

## Case Report

# A CASE SERIES OF CHILDREN WITH HIGH-RISK METASTATIC NEUROBLASTOMA TREATED WITH A NOVEL TREATMENT STRATEGY CONSISTING OF POSTPONED PRIMARY SURGERY UNTIL THE END OF SYSTEMIC CHEMOTHERAPY INCLUDING HIGH-DOSE CHEMOTHERAPY

**Yoshiko Hashii, MD, PhD, Takeshi Kusafuka, MD, PhD, Hideaki Ohta, MD, PhD, Akihiro Yoneda, MD, PhD, and Yuko Osugi, MD, PhD** □ *Departments of Pediatrics and Pediatric Surgery, Osaka University Graduate School of Medicine, Osaka, Japan*

**Yasutsugu Kobayashi, MD, PhD** □ *Department of Pathology, Osaka City General Hospital, Osaka, Japan*

**Masahiro Fukuzawa, MD, PhD, and Junichi Hara, MD, PhD** □ *Departments of Pediatrics and Pediatric Surgery, Osaka University Graduate School of Medicine, Osaka, Japan*

□ *The aim of this study was to clarify the feasibility of a novel treatment strategy consisting of postponed primary surgery till the end of systemic chemotherapy including HDC without interruption by local therapy for neuroblastoma patients at a high risk for relapse. After induction chemotherapy, patients received double conditioning HDC consisting of thiotepa and melphalan. Radical surgery was applied to local lesions. Irradiation was not applied to any lesions. Eleven consecutive pediatric neuroblastoma patients were treated according to this strategy. Seven of 11 patients remained in complete remission for 21[171 months. This treatment strategy seems feasible and a further study is warranted.*

**Keywords** delayed primary surgery, high-dose chemotherapy, high-risk neuroblastoma, melphalan, thiotepa

Advanced neuroblastoma is a systemic disease that spreads to the whole body, including the bone marrow, liver, lymph nodes, and bones. Morphologic or radiologic methods only detect metastases larger than a certain size. This indicates that high-risk neuroblastoma should be considered as a

Received 16 April 2007; accepted 19 March 2008.
We thank Yutaka Hamasaki, Shizuoka Children's Hospital, for histological review.
Address correspondence to Dr. Yoshiko Hashii, Department of Pediatrics, Osaka University Graduate School of Medicine, 2-2, Yamadaoka, Suita, Osaka 565-0871, Japan E-mail: yhashii@ped.med.osaka-u.ac.jp

systemic disease and that an increase of chemotherapy intensity is a premise for the improvement of treatment outcome. Indeed, the only method that has been proven to significantly improve survival is strengthening of chemotherapy intensity, including high-dose chemotherapy (HDC) with stem cell rescue. Thus, HDC with stem cell salvage following intensive induction chemotherapy has been widely accepted as being required for neuroblastoma treatment in high-risk groups, and treatment results have improved [1–5]. However, the 5-year event-free survival (EFS) rate is 30–40% and remains unsatisfactory despite various intensive efforts [3–5].

Neuroblastoma cells acquire resistance to chemotherapy in the early stages of treatment: it is therefore a premise for attaining a cure to eradicate tumor cells before they acquire chemotherapy resistance. We therefore assumed that interruption of systemic chemotherapy and/or reduction of dose intensity by surgery and radiotherapy might promote acquisition of drug resistance by malignant cells and clonal evolution. We also assumed that intensive chemotherapy combined with potent HDC might enable us to postpone local therapy until after the completion of all systemic chemotherapies. Based on this hypothesis, we postponed local therapy until the completion of all systemic chemotherapies, which made it possible to administer intensive chemotherapy in a shorter period of time and increase chemotherapy intensity without interruption of chemotherapy. As local therapy, surgery for the primary focus and residual metastases was finally performed at completion of treatment and response to chemotherapy was then evaluated pathologically.

With respect to local therapy, no difference has been observed in the EFS rate between gross total resection and partial resection in prospective studies despite a decrease in local recurrence rate with gross total resection [6, 7]. In a similar manner, local radiotherapy has been clearly shown to reduce local recurrence [8], but its contribution to the improvement of EFS has not been proven [9, 10]. Thus, though extensive local therapy reduces the local recurrence rate, it does not significantly contribute to increased survival. Since we assumed the significance of local surgery might increase under sufficient control of systemic disease, gross total resection was attempted in all patients. Radiotherapy was not performed because of the acute adverse effects and late complications following intensive chemotherapy. We report the results of this novel treatment approach in a consecutive series of 11 children (1992–2005) with high-risk abdominal neuroblastoma.

## PATIENTS AND METHODS

### Patients

Eleven consecutive pediatric patients with abdominal and mediastinum neuroblastoma at high risk for relapse were treated according to the

current treatment strategy. The high-risk category includes International Neuroblastoma Staging System (INSS) stage 4 for patients aged ≥1 year and MYCN$^+$ stage 4 for those aged <1 year. Table 1 summarizes the clinical data for the 11 patients (6 males; 1 aged <1 year; age range 6–64 months (median, 33 months)). Amplification of the MYCN gene was analyzed in primary tumors at first surgery in 8 patients and in bone marrow samples for the other 3. Six patients had MYCN amplification and 5 had no amplification by fluorescence in situ hybridization analysis. Seven of 8 patients who underwent biopsy of primary tumor or metastatic lymph nodes had unfavorable histopathological findings. Eight patients had poorly differentiated neuroblastoma and 1 had undifferentiated neuroblastoma according to the International Neuroblastoma Pathology Classification. Three patients (#6, #8, and #11) did not undergo biopsy at the outset but histological confirmation was performed in patient 6 at final surgery.

## Induction Chemotherapy

For induction chemotherapy, we basically employed the new A1 regimen (cyclophosphamide (CPA) 1.2 g/m$^2$, etoposide (VP-16) 100 mg/m$^2$ × 5, tetrahydropyraniyl-adriamycin (THP-ADR) 40 mg/m$^2$, and cisplatin (CDDP) 90 mg/m$^2$) or the 98A3 regimen (CPA 1.2 g/m$^2$ × 2, CDDP 90 mg/m$^2$, THP-ADR 40 mg/m$^2$, and vincristine (VCR) 1.5 mg/m$^2$). We administered newA1 or 98A3 regimen every 4 weeks. Three patients received carboplatin (CBDCA) instead of CDDP because of insufficient renal function. Irinotecan was additionally administered to 4 patients [11]. Induction chemotherapy was administered for 3–6 courses, principally until normalization of tumor markers (neuron-specific enolase (NSE), vanillyl-mandelic acid (VMA), and homovanillic acid (HVA)) and disappearance of distant metastases. The disappearance of metastasis was evaluated by computed tomography, technetium-99 bone scan, bilateral bone marrow aspiration, and iodine-123 metaiodobenzyl-guanidine scan.

## High-Dose Chemotherapy

After induction chemotherapy, patients received a double-conditioning regimen of 2 cycles of high-dose chemotherapy (HDC) consisting of thiotepa and melphalan [12]. Patients aged ≥2 years received 800–1000 mg/m$^2$ of thiotepa and 280–300 mg/m$^2$ of melphalan, and patients aged <2 years at HDC received 32 mg/kg of thiotepa and 6 mg/kg of melphalan. This HDC regimen consisted of 2 cycles of administration of thiotepa and melphalan with a 1-week interval; thiotepa (140–200 mg/m$^2$/day) and melphalan (50–75 mg/m$^2$/day) were administered on days −11, −10, -4 and −3. When creatinine clearance (Ccr) was <90 mL/min/1.73m$^2$ in

**TABLE 1** Characteristics of Patients with Stage 4 Neuroblastoma

| Patient | Age (mo.) | Gender | Primary site | INSS stage | Metastatic site at diagnosis | MYCN | Histology | |
|---|---|---|---|---|---|---|---|---|
| | | | | | | | INPC | Shimada |
| 1 | 25 | F | Adrenal | 4 | LN, B, BM | no amp | Poorly diff. NB | UH |
| 2 | 53 | M | Adrenal | 4 | LN, B | no amp | Poorly diff. NB + GN | UH |
| 3 | 20 | M | Adrenal | 4 | LN, B, BM, Lu | 14 | Undiff. NB | UH |
| 4 | 19 | M | Adrenal | 4 | LN, B | >20 | Poorly diff. NB | UH |
| 5 | 6 | M | Adrenal | 4 | LN, BM, L | 12 | Poorly diff. NB | FH |
| 6 | 48 | F | Adrenal | 4 | LN, B, BM | 20 | N.E | N.E |
| 7 | 29 | F | Adrenal | 4 | LN, B, BM | >10 | Poorly diff. NB | UH |
| 8 | 33 | M | Adrenal | 4 | LN, B, BM | >10 | N.E. | N.E. |
| 9 | 54 | M | Retroperitoneum | 4 | LN, B, BM | no amp | Poorly diff. NB | UH |
| 10 | 64 | F | Retroperitoneum | 4 | LN (mediastinum) | no amp | Poorly diff. NB | UH |
| 11 | 49 | F | Mediastinum | 4 | B, BM | no amp | N.E. | N.E. |

*Note.* B, bone; BM, bone marrow; F, female; FH, favorable histology; GN, ganglioneuroblastoma; INPC, International Neuroblastoma Pathology Classification; L, liver; LN, lymph node; Lu, lung; M, male; N.E., not evaluable; Poorly diff. NB, poorly differentiated neuroblastoma; UH, unfavorable histology; Undiff. NB, undifferentiated neuroblastoma.

**TABLE 2** Induction Chemotherapy and Preconditioning Regimens

| Patient | Conventional protocol | Chemotherapy (no. of courses) | Time to HDC from onset (days) | Time of stem cell harvest (course) | Stem cell source | Conditioning regimen | |
|---|---|---|---|---|---|---|---|
| | | | | | | Thiotepa ($mg/m^2$) | Melphalan ($mg/m^2$) |
| 1 | new A1[a] | 3 | 120 | 3 | Auto-BM | 1000 | 300 |
| 2 | new A1 | 5 | 130 | 2 | Auto-PB | 800 | 280 |
| 3 | new A1[a]/ CPT-11 | 6 | | N.D. | N.D. | | |
| 4 | new A1[a] | 5 | 167 | 3 | Auto-BM | 1000 | 280 |
| 5 | 98A3 / CPT-11 | 6 | 185 | N.D | u-CB | 26[c] | 6[b,c] |
| 6 | 98A3 / CPT-11 | 5 | 165 | N.D | u-CB | 760[b] | 210[b] |
| 7 | 98A3→98A3/ CPT-11 | 4 | 139 | 2 (PB) and 4 (BM) | Auto-PB, BM | 800 | 280 |
| 8 | 98A3 | 5 | 167 | 5 | Auto-BM | 800 | 280 |
| 9 | 98A3 | 4 | 167 | 2 | Auto-PB | 720[d] | 252[d] |
| 10 | 98A3 | 4 | 132 | 1 | Auto-PB | 720[d] | 252[d] |
| 11 | 98A3 | 4 | 148 | 3 (PB) and 4 (BM) | Auto-PB, BM | 570[d] | 200[d] |

*Note.* Auto-BM, autologous bone marrow; Auto-PB, autologous peripheral blood; CBDCA, carboplatin; CDDP, cisplatin; CPT-11, irinotecan N.D., not done; u-CB, unrelated cord blood.

[a]CBDCA was administered instead of CDDP.

[b]Drug dose was reduced because of transplantation from allogeneic donors.

[c]Drug was administered in terms of body weight (mg/kg).

[d]Drug dose was reduced to 70–90% of the prescribed dose according to renal function.

patients aged ≥2 years, dosage was adjusted according to the following formula: given dose ($mg/m^2$) = (Ccr/100) × 800 $mg/m^2$ (thiotepa) or 280 $mg/m^2$ (melphalan). In the case of allogeneic transplantation, doses of these drugs were reduced, because of severe gastrointestinal toxicity due to these alkylating agents. Peripheral blood stem cells (PBSCs) and bone marrow cells were used as salvage stem cells in 4 and 3 patients, respectively. Because PBSC count was insufficient for stem cell rescue in 2 patients, bone marrow cells were also transfused with PBSCs. Autologous bone marrow was used in the patients in whom PBSCs could not be harvested: this was performed at the end of induction chemotherapy. PBSCs were harvested after the 1st to 4th course of induction chemotherapy, after morphologic disappearance of tumor cells from bone marrow. In the 2 patients in whom disappearance of tumor cells from bone marrow was delayed, unrelated umbilical cord blood was used (Table 2).

### Local Therapy

After all courses of chemotherapy including HDC, radical surgery was finally applied to remove tumor tissue in local lesions when bone marrow function was acceptably recovered for surgery. Total resection for primary tumor as well as lymph node metastases was attempted. All lesions where the primary tumor and local lymph node metastases existed in onset of the disease were explored and if any suspected tumor tissue was existed, then resection was performed.

CT scan was performed after surgery to confirm no residual tumor in local lesions in all cases. Irradiation was not applied to any local lesions.

## RESULTS

### Response to Induction Chemotherapy

In 1 patient (#3), tumors did not respond to induction chemotherapy and he showed progressive disease. He died from progression of pulmonary metastatic tumors 6 months after diagnosis before HDC. After 3–6 courses (median, 5 courses) of induction chemotherapy, 10 patients received HDC. Time from initial diagnosis to HDC was 4–6 months (median, 5 months). With respect to metastases at initial diagnosis in patients who received HDC, these were detected in bone ($n = 8$), bone marrow ($n = 7$), lymph node ($n = 9$), and liver ($n = 1$)and evaluated by computed tomography, technetium-99 bone scan, bilateral bone marrow aspiration, and iodine-123 metaiodobenzyl-guanidine scan. After induction chemotherapy, the bone marrow metastases disappeared in all patients, but liver and bone metastases each remained in 1 patient, respectively. Primary tumors and regional lymph node metastases remained in all patients. Tumor marker levels were

normalized in all patients. At HDC, 7 patients attained PR and 2 VGPR according to International Neuroblastoma Response Criteria.

## Response to High-Dose Chemotherapy

Nine patients received HDC at PR or VGPR. The size of one primary tumor did not change. After HDC, residual bone metastases disappeared in 1 patient. Liver metastases persisted in 1 patient. Five primary tumors that decreased to below 50% after conventional chemotherapy decreased to below 10% and the sizes of primary tumors did not change dramatically, but metastatic lymph nodes disappeared in 2 patients. With respect to adverse reactions observed during HDC, fungal osteomyelitis was observed in 1 patient who received allograft. In addition, gastrointestinal tract mucositis with bloody stools was observed in 1 patient and NCI-CTC grade III mucositis was noted in all patients.

## Surgery and Pathological Evaluation of Tumors

Radical surgery was performed in each patient, resecting all recognizable lesions, including the primary tumor and affected lymphatic tissues. The timing of surgery was 2 months after the initiation of HDC in most patients who received autologous stem cell transplantation, and it was prolonged to 4 months in the patients who underwent allogeneic transplantation and/or had HDC-related complications (Table 3).

We evaluated the effect of chemotherapy including HDC by comparing tumor specimens resected at outset and second-look surgery in 6 patients, according to the histologic criteria for the effects of anticancer therapy for pediatric solid malignant tumors in Japan (Table 4) [13]. We were not able to evaluate the remaining 4 patients as insufficient amounts of pretreatment specimen were available. Necrotic or fibrous lesions were seen in one-third to two-thirds of the area of tumor tissues (Ef1b) of 1 patient. In the 4 cases, prominent necrosis and loss of tumor cells were observed in more than two-thirds of the tumor area and was associated with fibrosis and calcification (Ef2). On histological examination, the specimens from almost all, except one (#11), resected primary tumors had some degree of residual tumor tissue and in occasional cases viable tumor tissue was recognized in concurrently resected lymph nodes. However, residual tumor tissue consisted of scattered nests of neuroblastic cells in degenerative fibrous tissue, occasionally associated with Schwannian cell proliferation. Neuroblastic cells were more differentiating with abundant neutrophil formation as compared to pretreatment tumors. The preoperative induction chemotherapy and HDC produced remarkable cytotoxic effects and induced differentiation toward ganglionic cells. Examples of the histopathologic changes resulting from treatment are shown in Figures 1 and 2.

**TABLE 3** Response to Treatment and Outcome

| Patient | Response to induction chemotherapy | | | Response to induction chemotherapy and HDC | | | Time to surgery | | Post therapy histology classification[a] | Outcome from diagnosis (mo.) |
|---|---|---|---|---|---|---|---|---|---|---|
| | Response | Residual site | VMA,HVA (mg/mg$_{Cr}$)[c] | Response | Residual site | VMA, HVA (mg/mg$_{Cr}$)[c] | From HDC (days) | From onset (days) | | |
| 1 | PR | P/LN | ≦20, ≦20 | PR | P/LN | ≦20, ≦20 | 96 | 216 | N.E. | EFS (171) |
| 2 | PR | P/LN | N.E.[d] | VGPR | P | N.E.[d] | 79 | 209 | N.E. | EFS (104) |
| 3 | PD | – | | – | – | | –– | –– | – | PD (3[b]) |
| 4 | PR | P/LN/B | N.E.[d] | VGPR | P | N.E.[d] | 68 | 235 | Ef1b | EFS (159) |
| 5 | PR | L/LN | ≦20, ≦20 | PR | L/LN | ≦20, ≦20 | 106 | 291 | Ef2 | EFS (73) |
| 6 | PR | P/LN | N.E.[d], ≦20 | VGPR | P | N.E.[d] ≦20 | 99 | 264 | N.A | EFS (57) |
| 7 | PR | P/LN | N.E.[d], ≦20 | VGPR | P | N.E.[d], ≦20 | 52 | 191 | Ef2 | Relapse in LN (24) |
| 8 | VGPR | P | ≦20, ≦20 | VGPR | P | ≦20, ≦20 | 83 | 250 | N.E. | EFS (38) |
| 9 | VGPR | P | ≦20, ≦20 | VGPR | P | ≦20, ≦20 | 85 | 252 | Ef2 | Relapse in multiple sites (20) |
| 10 | PR | P | ≦20, ≦20 | VGPR | P | ≦20, ≦20 | 50 | 182 | Ef2 | Relapse in LN (18) |
| 11 | PR | P | ≦20, ≦20 | PR | P | ≦20, ≦20 | 55 | 203 | Ef3 | EFS (21) |

*Note.* B, bone; CR, complete response; EFS, event-free survival; HDC, high-dose chemotherapy; L, liver; LN, lymph node; NR, no response; P, primary; PD, progressive disease; PR, partial response; VGPR, very good partial response. HVA, urine homovanillic acid; VMA, urin vanillylmandelic acid.

[a]Pathological classification according to the Committee on Histological Classification of Childhood Tumors, Japanese Society of Pathology (see Table 4).

[b]Decreased.

[c]The level of VMA and HVA are revised by urin creatinin. Normal levels of VMA and HVA are below under 20 mg/mg Cr in our institute for every age.

[d]Normal levels of cathecholamine at onset.

**TABLE 4** Pathological Classification of Treatment Effect According to the Committee on Histological Classification of Childhood Tumors, Japanese Society of Pathology

| | |
|---|---|
| Ef0 | No effect |
| Ef1a | Necrosis of tumor cells in less than one-third of tumor area |
| Ef1b | Necrosis of tumor cells in less than two-thirds and in more than one-third of tumor area |
| Ef2 | Necrosis and disappearance of tumor cells plus calcification and fibrosis in more than two-thirds of tumor area |
| Ef3 | All tumors are affected by obvious necrotic tissue and no tumor cells are seen |

## Outcome

Altogether, 10 of 11 patients received HDC and 7 patients have remained in remission for 21–171 months (median, 73 months). In 2 patients (#7 and #10), the tumor relapsed in regional abdominal and thoracic lymph nodes after 24 and 18 months, respectively, from initial diagnosis. In patient #9, relapse was observed in multiple sites including bone, bone marrow, and lymph nodes 20 after from diagnosis. After gross total resection of the tumors, patient #7 received salvage chemotherapy, consisting of irinotecan and topotecan, and local irradiation. Finally, allogeneic stem cell transplantation preconditioned with fludarabine and busulfan was performed. She has been in remission for 21 months after relapse. The other 2 patients are currently undergoing treatment.

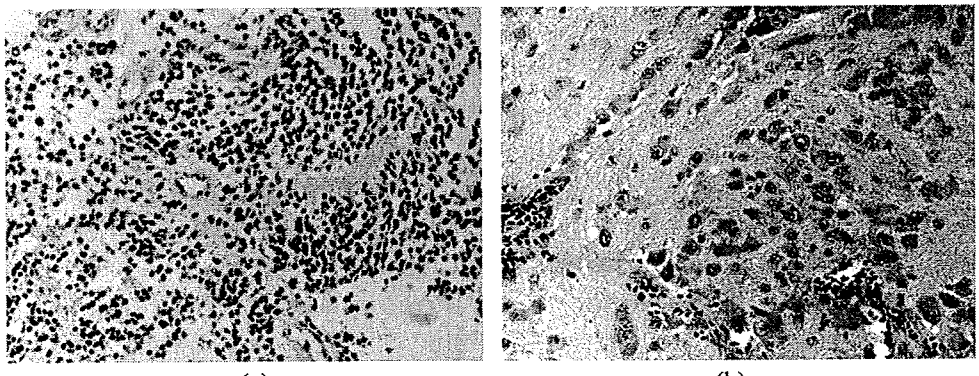

(a) (b)

**FIGURE 1** Histological findings for primary tumor is from patient 4: (a) before treatment—poorly differentiated subtype with low mitosis karyorrhexis index (MKI); and (b) after HDC—residual tumor nests of differentiating neuroblastic cells.

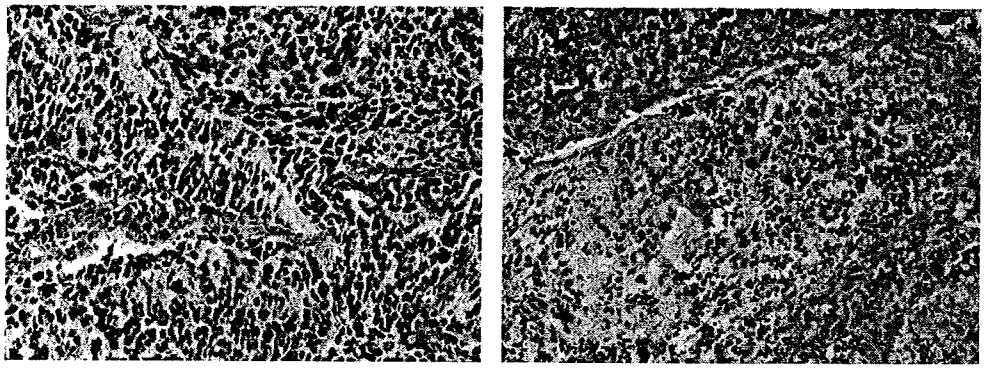

(a) (b)

**FIGURE 2** Histological findings for lymph node metastasis from patient 5: (a) before treatment—poorly differentiated subtype with low mitosis karyorrhexis index (MKI); and (b) after HDC—extensive necrosis with residual differentiating neuroblastic cell nests.

## DISCUSSION

Primary surgery is generally and traditionally performed between induction chemotherapy and HDC. It might be possible that tumor cells become more sensitive to chemotherapy after mass reduction, but the rationale of the timing of local therapy is unclear. In this case series, we performed primary surgery after completion of induction chemotherapy and HDC based on the hypothesis that consecutive conventional and high-dose chemotherapies without interruption by local therapy can eradicate systemically spread tumor cells before acquisition of resistance to cytotoxic drugs and clonal evolution of resistant clones. The disadvantage of this treatment strategy is the increased risk for metastasis of tumor cells residing in the local tumors and emergence of resistant clones in these. Among 11 consecutive high-risk patients with stage 4 neuroblastoma, except 1 patient whose tumors were primarily refractory to induction chemotherapy, none displayed progressive disease before local surgery; 7 patients remain in event-free survival; and systemic relapse was observed in only 1 patient.

The disadvantage of performing surgery during chemotherapy appears to be related to the interruption of systemic therapy. Furthermore, when intraoperative/postoperative complications occur, discontinuation of systemic chemotherapy may be prolonged and this may cause systemic relapse. In performing surgery after all courses of chemotherapy, the timing of surgery can be selected under conditions of sufficient tumor control. Surgery was safely performed after recovery of hematopoiesis in this series.

In this treatment strategy, HDC plays a key role, since less potent HDC may allow progression of the local tumor. For HDC, we employed a double-conditioning regimen consisting of thiotepa and melphalan, as previously reported [12]. These agents were chosen for the treatment of neuroblastoma, as they show efficacy as high-dose, single-agent therapy for